NBTIN BASED SIS MULTILAYER STRUCTURES FOR SRF APPLICATIONS *

A.-M. Valente-Feliciano#, G. Eremeev, H. L. Phillips, C. E. Reece, and J.K. Spradlin, Thomas Jefferson National Accelerator Facility, Newport News, VA 23606, U.S.A.
Q. Yang, Norfolk State University, VA 60439, U.S.A.
D. Batchelor, North Carolina State University, Raleigh, NC 27695, U.S.A.
R.A. Lukaszew, College William & Mary, VA 23185, U.S.A.

Abstract

For the past three decades, bulk niobium has been the material of choice for SRF cavities applications. RF cavity performance is now approaching the theoretical limit for bulk niobium. For further improvement of RF cavity performance for future accelerator projects, Superconductor – Insulator - Superconductor (SIS) multilayer structures (as recently proposed by Alex Gurevich) present the theoretical prospect to reach RF performance beyond bulk Nb, using thinly layered higher-Tc superconductors with enhanced H_{c1}. Jefferson Lab (JLab) is pursuing this approach with the development of NbTiN and AlN based multilayer SIS structures. This paper presents the results on the characteristics of NbTiN films and the first RF measurements on NbTiN-based multilayer structure on thick Nb films.

SIS MULTILAYER APPROACH FOR SRF CAVITIES

A few years ago, a concept was proposed by A. Gurevich [1] which would allow taking advantage of high-Tc superconductors without being penalized by their lower Hc_1. The idea is to coat superconducting radio-frequency (SRF) cavities with alternating superconducting and insulating layers (SIS structures) with a thickness d smaller than the penetration depth λ (figure 1). If the superconducting film is deposited with a thickness d <<λ, the Meissner state can be retained at a magnetic field much higher than the bulk H_{c1}. The strong increase of H_{c1} in films allows utilization of RF fields higher than the critical field H_c of Nb but lower than those at which the flux penetration may create a problem. The thin higher-Tc layers provide magnetic screening of the bulk superconducting cavity preventing vortex penetration. The BCS resistance is also strongly reduced because the superconducting materials used have higher gap Δ (Nb_3Sn, NbTiN …) than Nb. With such structures, Q-values at 4.2 K could be increased two orders of magnitude above Nb values.

If a 50 nm Nb_3Sn layer is coated on a bulk Nb cavity with an insulating interlayer and if the Nb cavity can sustain fields up to 150mT, this structure could potentially sustain external magnetic fields of about 320mT and therefore reach accelerating gradients without precedent.

*Authored by Jefferson Science Associates, LLC under U.S. DOE Contract No. DE-AC05-06OR23177. The U.S. Government retains a non-exclusive, paid-up, irrevocable, world-wide license to publish or reproduce this manuscript for U.S. Government purposes.
#valente@jlab.org

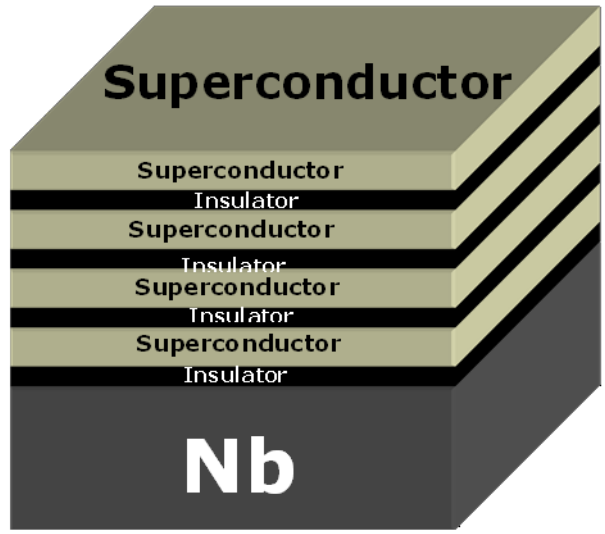

Figure 1: The SIS multilayer concept.

CANDIDATE MATERIALS

Superconductor: NbTiN

Although A15 compounds such as Nb_3Sn have a higher T_c, the Nb B1-compounds are less sensitive to radiation damage and crystalline disorder.

B1-compounds have a NaCl structure where metallic atoms form a face centred cubic (fcc) lattice and non-metallic atoms occupy all the octahedral interstices. These compounds are characterized by the fact that they always have a certain amount of vacancies, usually distributed randomly throughout the lattice [2]. The superconducting properties of B1 compounds are very sensitive to deviation from stoichiometric composition.

The ternary nitride NbTiN is the B1-compound with the highest critical temperature, 17.8 K.

The phase diagram of the binary system Nb-N up to N/Nb=1 includes many different phases [3, 4], characterized by different Tc [5]. The B1-NbN superconducting phase of interest (cubic δ-phase, a=4.388 Å) is only thermodynamically metastable at room temperature. The Tc is very sensitive to the nitrogen (N) stoichiometry and NbN suffers from a high resistivity due to the presence of both metallic and gaseous vacancies randomly distributed in both sub-lattices, in amount of 1.3% respectively. The equi-atomic composition is $Nb_{0.987}N_{0.987}$[6].

The ternary nitride NbTiN presents all the advantages of NbN and exhibits increased metallic properties with higher titanium (Ti) percentage. Ti is a good nitrogen getter, so the higher the Ti composition, the lower the number of vacancies. In contrast with NbN, the B1-TiN phase is stable at room temperature (Tc=5 K, a=4.24 Å). The two nitride phases are completely miscible resulting in a superconducting ternary NbTiN cubic phase which remains thermodynamically stable at room temperature [7]. The Tc is slightly higher for NbTiN but as for NbN, N stoichiometry is critical to obtaining the right superconducting phase.

Some of the common techniques used to produce NbTiN are reactive magnetron sputtering [8] and high impulse magnetron sputtering [9].

Insulator: AlN

AlN is an insulator that is extensively used for its dielectric and piezo-electric properties for multilayer terra-hertz (THz) mixers and surface acoustic wave sensors. It can be grown with a wurtzite (hexagonal close-packed, a=3.11 Å, c=4.98 Å) or sphalerite (B1 cubic, a= 4.08 Å) structure (figure 3).

AlN has been found to enhance the superconducting properties, such as T_c, of NbN and NbTiN, in particular for very thin films [10]. AlN's thermal conductivity (3.19 W/cm2 at 300 K) is comparable to Cu (4.01 W/cm2).

EXPERIMENTAL METHOD

This study uses an ultra-high vacuum (UHV) multi-technique deposition system tailored to in-situ multilayer depositions and described elsewhere [12].

Multiple sample holders are available on the main chamber to allow the simultaneous deposition of witness samples to probe the quality and properties of the individual layers and allow the variation of deposition parameters during the same deposition run. All sample stages can be heated up to 800 °C and are equipped with shutters to allow the deposition in the same run of multiple sets of samples with different parameters, ensuring directly comparable environmental conditions.

NbTiN films are grown on various substrates (Nb, MgO (100), AlN ceramics) and at various temperatures by DC reactive sputtering with an 80w. % Nb/ 20w. % Ti target. Table 1 summarizes the typical coating parameters and properties for NbTiN films.

Table 1: Tc for NbTiN Films at Various Coating Temperature

	NbTiN
N_2/Ar	0.23
Total Pressure [Torr]	$2x10^{-3}$
Sputtering Power [W]	300
Deposition rate [nm/min]	22

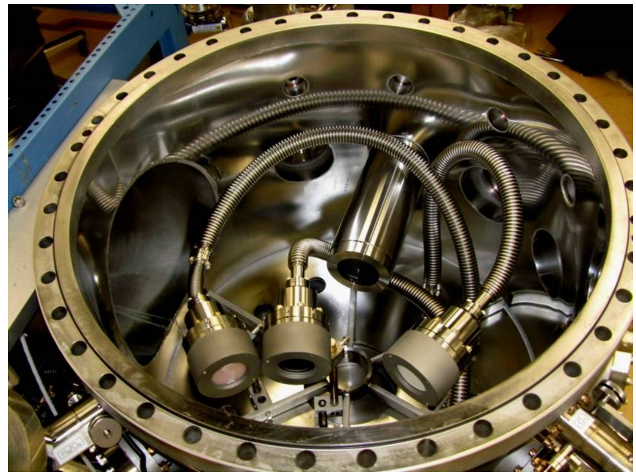

Figure 2: Setup in the UHV multi-technique deposition system main chamber.

AlN films are produced with reactive sputtering of an elemental Al (99.999%) target. The AlN films are fully transparent and exhibit the B1 cubic structure. The corresponding deposition conditions are reported in table 2.

Table 2: Coating Parameters for AlN

	AlN
N_2/Ar	0.33
Total Pressure [Torr]	$2x10^{-3}$
Sputtering Power [W]	100
Deposition rate [nm/min]	3

The films produced are then analysed with different techniques. The crystallographic characteristics of the layers are probed via by θ-2θ x-ray diffraction with Cu $K\alpha$ radiation. T_c measurements are conducted via the four-point probe method on a multi-sample measurement setup using calibrated CERNOX thermometer s (sensitivity: 50 mK). RF measurements are conducted on 50 mm disk samples coated simultaneously with a 7.5 GHz TE011 sapphire loaded cavity (SIC) [10].

NBTIN FILMS

The substrate dependence of the crystallographic structures of NbTiN films by XRD analysis was investigated. The films deposited on crystalline substrate such as MgO (100), Al2O3 (1-210) and epitaxial w-AlN (0001) on sapphire exhibit relatively good structure [11]. Good quality films with a structure corresponding to the δ-phase are produced with various thicknesses. The results are reported in figure 3 and table 3 for films deposited on MgO (100). The best T_c, 16.95 K, was obtained for a 1.6 μm NbTiN film. H_{c1} measurements by Squid magnetometry are also under way on this series of films.

ISBN 978-3-95450-143-4

Table 3: Transition temperatures as a function of thickness for NbTiN films grown on MgO (100).

NbTiN/MgO (100)			
Thickness [nm]	T_c [K]	ΔT_c [K]	a_0 [Å]
10	12.11	0.91	4.3487
35	16	0.39	
50	15.97	0.16	4.3644
100	16.57	0.21	4.3657
1625	16.95	0.06	4.3618

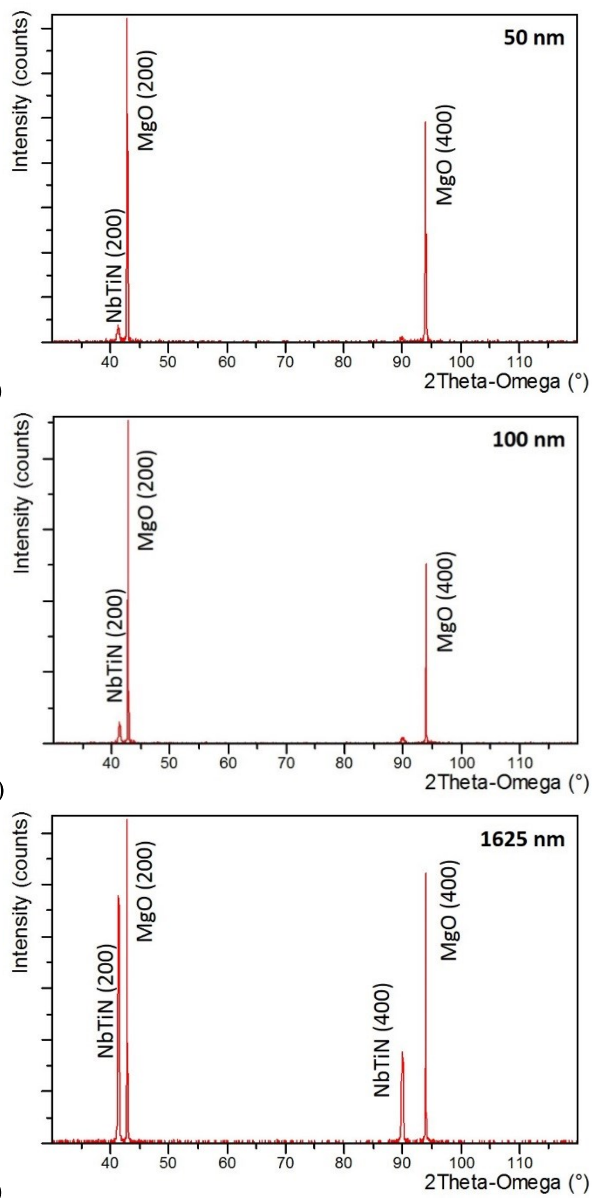

Figure 3: XRD Bragg-Brentano (θ–2θ) spectra for NbTiN coated on MgO (100) with a thickness of (a) 50 nm, (b) 100 nm and (c) 1.6 µm.

NbTiN/AlN STRUCTURES

SIS structures based on NbTiN and AlN have been coated at 450°C in-situ on bulk Nb and Nb/a-Al_2O_3 substrates after a 24 hour-bake at 600 °C. The samples are then annealed at 450 °C for 4 hours.

NbTiN/AlN on Nb Thick Film

Figure 4 shows the surface resistance measurement of an NbTiN/AlN structure coated on a thick Nb film. The film used as a substrate was coated ex-situ by energetic condensation [11]. The multilayer structure shows a suppressed T_c of about 8 K for the Nb film where it was previously measured at 9.3 K. This is most likely due to oxygen diffusion resulting from the oxide layer reduction during the 600 ˚C bake-out. Other multilayer structures have been coated on ECR films previously characterized with the SIC setup at lower bake-out and coating temperatures and are waiting to be measured. To avoid the diffusion of oxygen into the Nb film during bake-out, one can remove the Nb oxide layer by in-situ plasma etching. Another solution is to coat both the Nb film and SIS structure in-situ. This will be implemented in the near future.

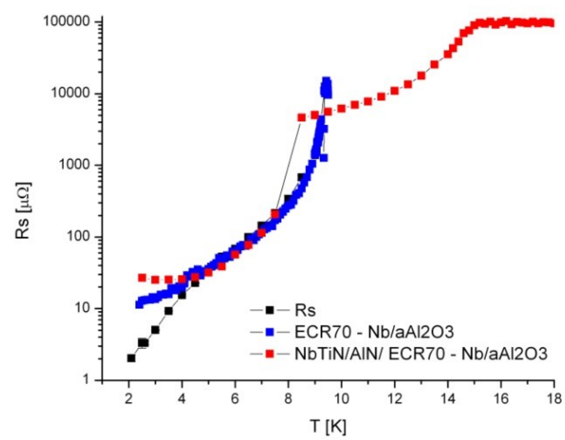

Figure 4: Surface resistance as a function of temperature for NbTiN/AlN structure coated on ECR Nb film measured in the SIC setup.

NbTiN/AlN on Bulk Nb Substrate

A similar structure was deposited on a single crystal bulk Nb substrate. The structure was examined by θ-2θ x-ray diffraction with Cu $K\alpha$ radiation. The scan shows reflections for Nb (100) and (200), AlN (111) and NbTiN (111). The lattice parameters a_0 are respectively 3.301 Å, 4.041 Å and 4.330 Å for Nb, AlN and NbTiN.

ISBN 978-3-95450-143-4

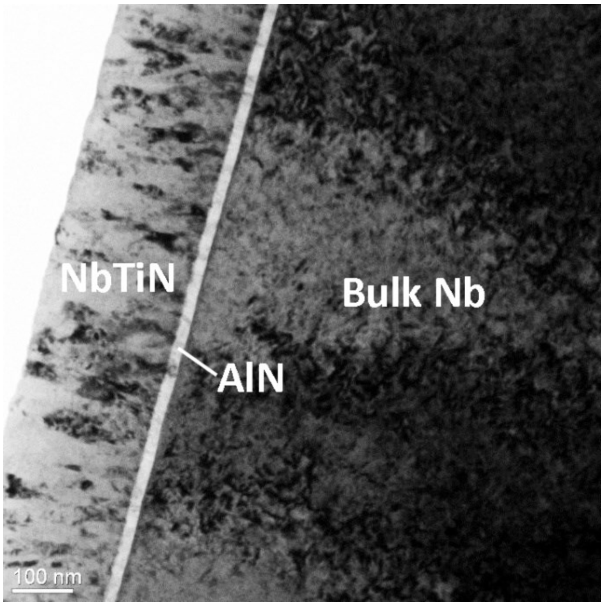

Figure 5: TEM image of a FIB cut NbTiN/AlN/Nb structure.

A cross-section sample has been cut by FIB (focused ion beam) and observed by TEM. The TEM cross section (figure 5) reveals polycrystalline NbTiN and AlN layers with sharp interfaces.

Figure 6 shows the loaded quality factor for the SIC measurement with the NbTiN/AlN/Nb bulk sample. It reveals two transitions at about 9.2 K for bulk Nb as expected and at 16 K the NbTiN layer. Further measurements are on the way for the surface resistance of this sample [13].

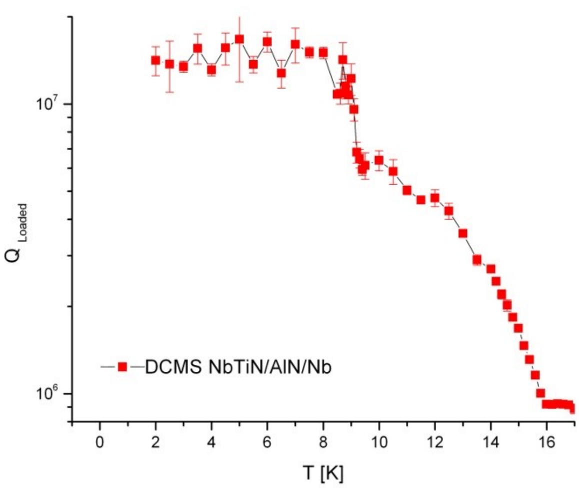

Figure 6: Quality factor as a function of temperature for NbTiN/AlN/Nb (bulk) measured in the SIC setup.

CONCLUSION

- JLab in collaboration with surrounding universities (College William & Mary, Old Dominion University, and Norfolk State University) is pursuing the opportunity to create SIS multilayer structures following the concept proposed by A. Gurevich for overcoming the fundamental bulk material limitation, H_{c1}. This has the potential to create viable superconducting RF cavity surfaces that will reduce the cost framework of SRF accelerators, reach higher gradients, and allow operation of SRF structures at 4K.
- Good quality NbTiN and AlN films have been produced by DC reactive sputtering. The first multilayer structures have been deposited and are under analysis.
- NbTiN based multilayer structures are analysed on thick Nb films and Nb bulk.

AKNOWLEDGEMENT

The authors are very grateful for the support from all the technical staff at Jefferson Lab. The authors would also like to thank the William and Mary Characterization Facility in the ARC building at Jefferson Lab.

REFERENCES

[1] A. Gurevich, Appl. Phys. Lett. 88, 012511 (2006).
[2] S. V. Vonsovsky, Yu. A. Izyumov, E. Z. Kumaev, "Superconductivity of transition metals, their alloys and compounds", Springer-Verlag (1982).
[3] G. Brauer, J. Less-Common Metals 2 (1960) 131.
[4] R.W. Guard, J.W. Savage and D.G. Swarthout, Trans. Metall. Soc. ATME 239 (1967) 643.
[5] L. Toth, Transition Metal Carbides and Nitrides (Academic Press, New York, 1971), chap. 7.
[6] V. Palmieri, 10th Workshop on RF Superconductivity Proceedings, Tsukuba 2001 (Noguchi) 162-169.
[7] C. Benvenuti et al. Nucl. Instrum. Methods B 124 (1997) 106-111.
[8] A. Nigro et al., Adv. Cryog. Eng. 34, 813 (1988).
[9] Y.P. Purandare, A.P. Ehiasarian, and P. Eh. Hovsepian, J. Vac. Sci. Technol. A 26(2) 288, (2008).
[10] B. Xiao, Rev. Scient. Instr. 82, p056104 (2011).
[11] A-M Valente-Feliciano et al., THPO074 Proceedings of Superconducting RF conference 2011, Chicago, July 2011.
[12] A-M Valente-Feliciano, TUIOB06, Proceedings of Superconducting RF conference 2011, Chicago, July 2011.
[13] G. Eremeev, TUP070, these proceedings.

ISBN 978-3-95450-143-4